Supporting Information for

Sulfur-Bridged Iron-Polyphthalocyanine on Cu$_x$O/Copper Foam: Efficient and Durable Electrocatalyst for Overall Water Splitting

Xinran Chen,[a] Yang Li,[a] Lu Chen,[a] Lili Cui,[a] Zhiyu Dou,[a] Xingquan He,[*a] Meihong Fan[*a] and Tewodros Asefa[*b]

[a] School of Chemistry and Environmental Engineering, Changchun University of Science and Technology, 7089 Weixing Road, Changchun, Jilin 130022, P. R. China
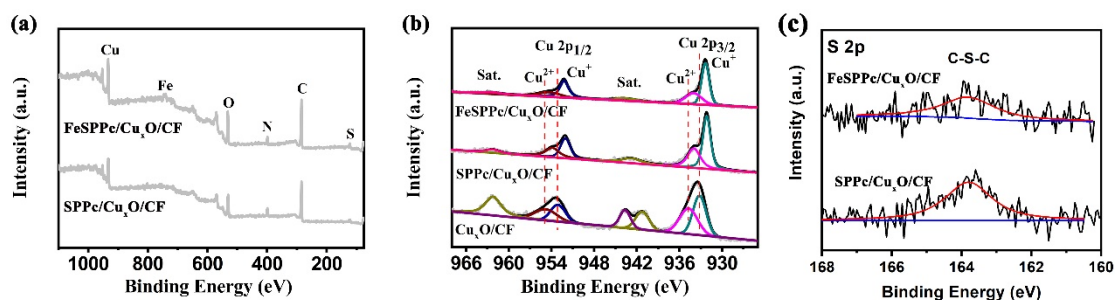
[b] Department of Chemistry and Chemical Biology & Department of Chemical and Biochemical Engineering Rutgers, The State University of New Jersey, 610 Taylor Road, Piscataway, New Jersey 08854, USA
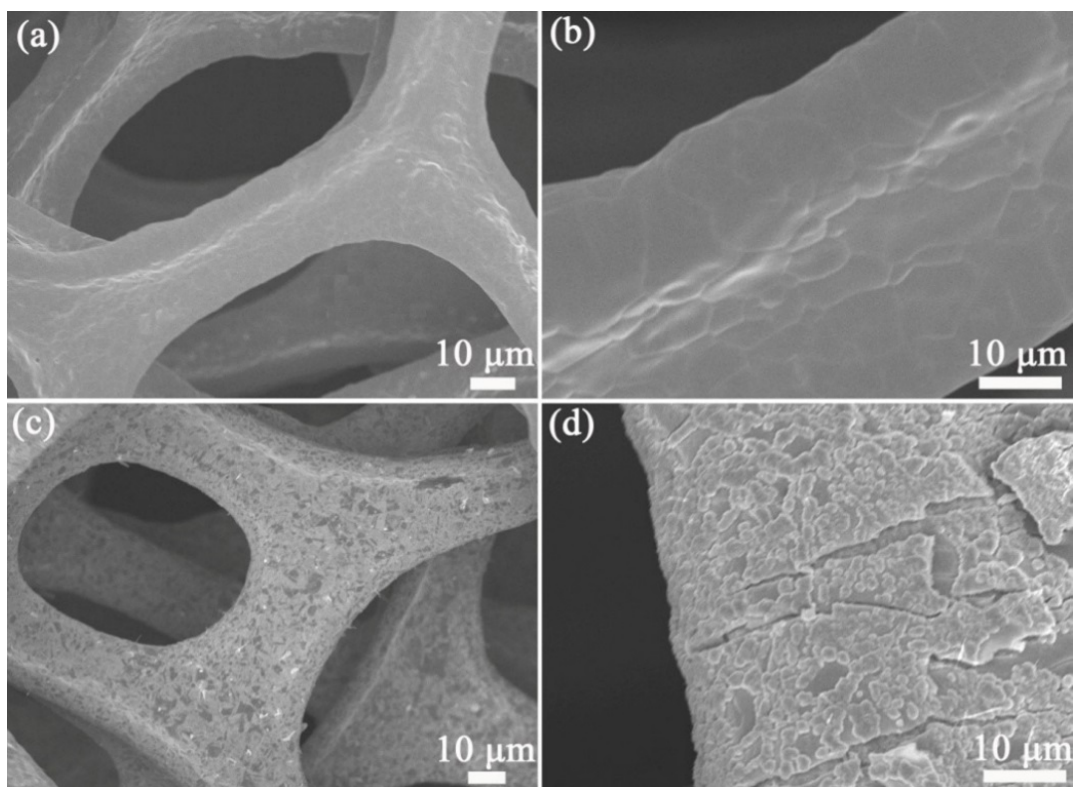
Figure S1. (a-d) SEM images of (a,b) CF and (c,d) Cu_xO/CF.
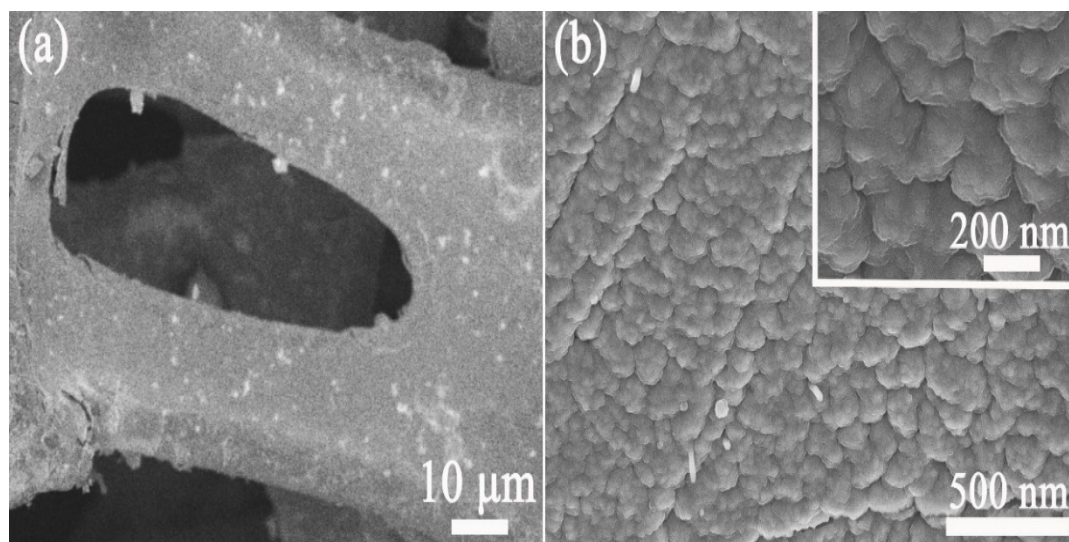
Figure S2. SEM images of $SPPc/Cu_xO/CF$ in different magnifications.

Figure S3. (a) Survey XPS spectra of FeSPPc/Cu$_x$O/CF and SPPc/Cu$_x$O/CF. (b) High-resolution XPS spectra of Cu 2p peak for Cu$_x$O/CF, SPPc/Cu$_x$O/CF and FeSPPc/Cu$_x$O/CF. (c) High-resolution XPS spectra of S 2p peak for SPPc/Cu$_x$O/CF and FeSPPc/Cu$_x$O/CF.

Table S1. Relative amounts (at.%) of the different elements on the surfaces of the materials investigated in the work. The analysis is done based in their XPS spectra.

Catalyst / Amounts (at.%)	C	N	O	S	Fe	Cu
FeSPPc/Cu$_x$O/CF	62.17	7.03	17.46	1.44	4.77	7.13
SPPc/Cu$_x$O/CF	65.9	8.04	18.4	1.89	-	5.78
Post-HER	50.66	4.27	25.03	2.75	5.70	11.59
Post-OER	41.06	2.11	30.08	1.88	7.56	17.30

Table S2. Comparison of the electrocatalytic activities the materials studied for HER and OER among each other and with respect to benchmark noble metal HER and OER catalysts.

Catalysts	HER		OER	
	η_{10} (mV)	η_{100} (mV)	η_{10} (mV)	η_{100} (mV)
FeSPPc/Cu$_x$O/CF	38	298	350	471
SPPc/Cu$_x$O/CF	61	349	410	572
Cu$_x$O/CF	52	393	414	594
CF	139	518	441	682
Pt/C/Cu$_x$O/CF	11	162	-	-
RuO$_2$/Cu$_x$O/CF	-	-	370	540

η_{10}: The overpotential required by the material to electrocatalyze the reaction at 10 mA cm^{-2}.

η_{100}: The overpotential required by the material to electrocatalyze the reaction at 100 mA cm^{-2}.
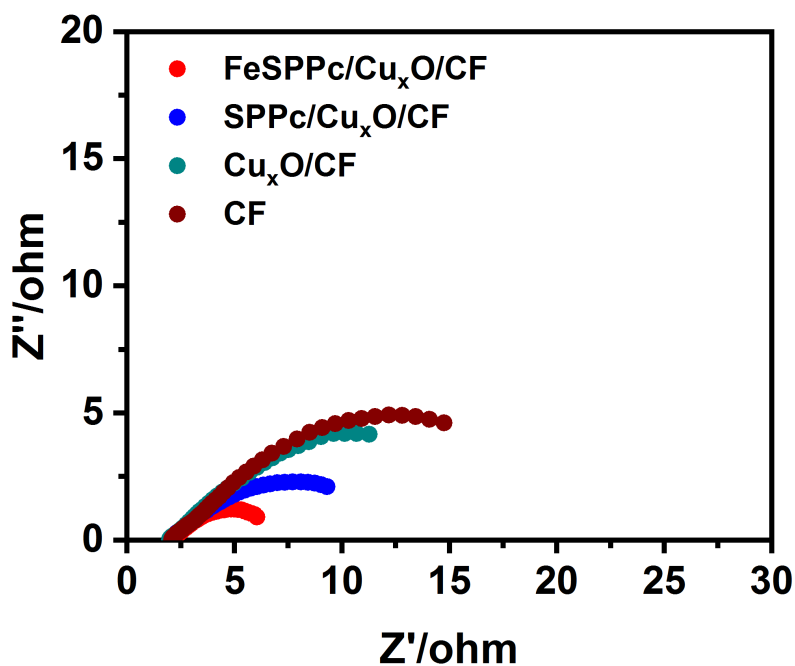
Figure S4. Nyquist plots for the electrocatalysts in KOH electrolyte (1 M) under anodic bias that drives rapid oxygen evolution.

According to previous reports, double layer capacitance (C_{dl}) is proportional to the effective electrode surface area of the materials and can be extracted from the difference in the plots of current density (J) between the anodic and cathodic sweeps versus can rate. Based on the curves, the values of C_{dl} of FeSPPc/Cu$_x$O/CF, SPPc/Cu$_x$O/CF, Cu$_x$O/CF, and CF are determined to be 28.8, 23.7, 17.4, and 5.6 mF cm^{-2}, respectively (Figure 5b in the main text). To estimate the electrochemically active surface area (ECSA), a specific capacitance (C_s) value of 0. 060 mF/cm^2 in 1 M KOH is adopted. Then, the value of ECSA for each material is calculated with the following equation (Eqn. 1):

$$\text{ECSA} = \frac{C_{dl}}{C_s} \times \text{ASA} \qquad \qquad \text{Eqn. 1}$$

where C_s is the specific capacitance of the sample and ASA is the actual surface area of the electrode. In this work, the value of C_s is estimated to be 0.06 mF/cm^2. Accordingly, the values of ECSA of FeSPPc/Cu$_x$O/CF, SPPc/Cu$_x$O/CF, Cu$_x$O/CF, and CF are found to be 120, 98.75, 72.5, and 23.3 cm^2, respectively. The results are compiled in Table S3.

Table S3. The values of C_{dl} and R_{ct} of the electrocatalysts or electrodes. The data are derived from their CV curves that are obtained with different scan rates and their equivalent circuit models.

Catalyst	C_{dl} (mF cm^{-2})	ECSA (cm^2)	R_{ct} for HER （Ω）	R_{ct} for OER （Ω）
FeSPPc/Cu$_x$O/CF	28.8	120.0	2.61	5.41
SPPc/Cu$_x$O/CF	23.7	98.75	3.83	11.97
Cu$_x$O/CF	17.4	72.5	4.80	18.02
CF	5.6	23.3	28.87	24.02
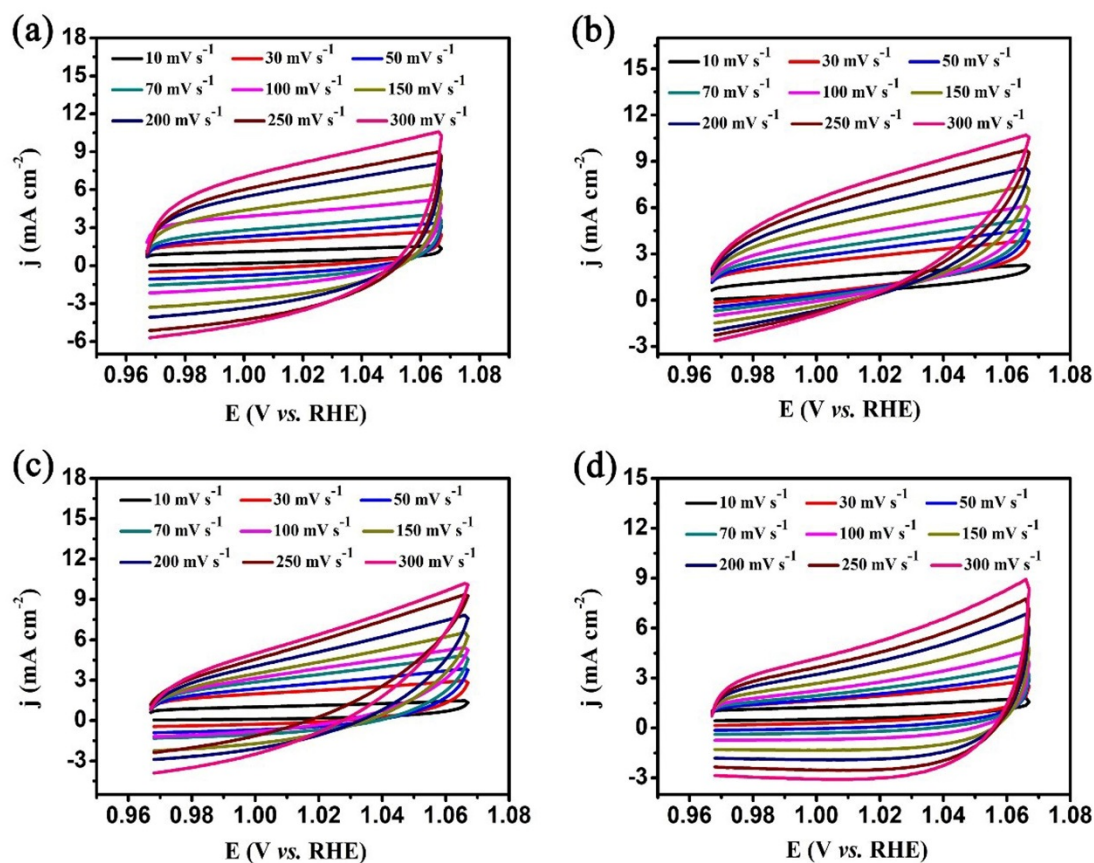
Figure S5. (a-d) CV curves for (a) FeSPPc/Cu$_x$O/CF, (b) SPPc/Cu$_x$O/CF, (c) Cu$_x$O/CF and (d) CF obtained at different scan rates of 10, 30, 50, 70, 100, 150, 200, 250, and 300 mV s^{-1} in the potential range from 0.97 to 1.07 V vs. RHE in 1 M KOH electrolyte saturated with N$_2$.
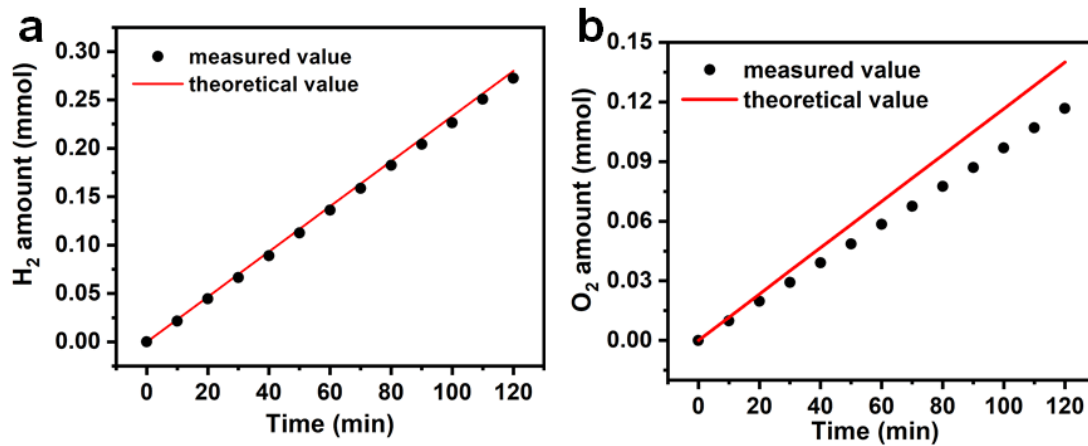
Figure S6. Efficiencies of (a) hydrogen and (b) oxygen production over FeSPPc/Cu$_x$O/CF under potentiostatic electrolysis in 1 M KOH solution for 2 h. The black dotted lines represent the theoretical amounts based on the measured current density, and the red curves represent the amount of determined experimentally.

We carried out Faradaic efficiency measurement of FePPc/Cu$_x$O/Cu in HER and OER by collecting H$_2$ and O$_2$ evolved *via* a water drainage method and their amounts (in mol) were then calculated using the ideal gas law. The purity of the gas evolved from the reaction was confirmed with gas chromatography (GC). The Faradaic efficiency was the calculated according to Eqn. 2 below:

$$\text{Faradaic efficiency} = \frac{\text{charges for gas evolution}}{\text{total charges generated}}$$

$$= \frac{n \times z \times F}{I \times t} \times 100\% \qquad \text{Eqn. 2}$$

where n is the amount of product detected (number of moles, mol), z is the number of electrons required to obtain 1 molecule of the product, F is the Faraday constant (96485 C mol^{-1}), I represents the current generated in the experiment and t is the time for gas collection.

Based on the amount of gas determined experimentally and expected theoretically, this material (FePPc/Cu$_x$O/Cu) is found to give ~100% Faradaic yield in HER and about 87% yield in OER. The Faradaic efficiency is lower than 100% in OER probably the partial dissolution of oxygen in alkaline electrolyte.[1]
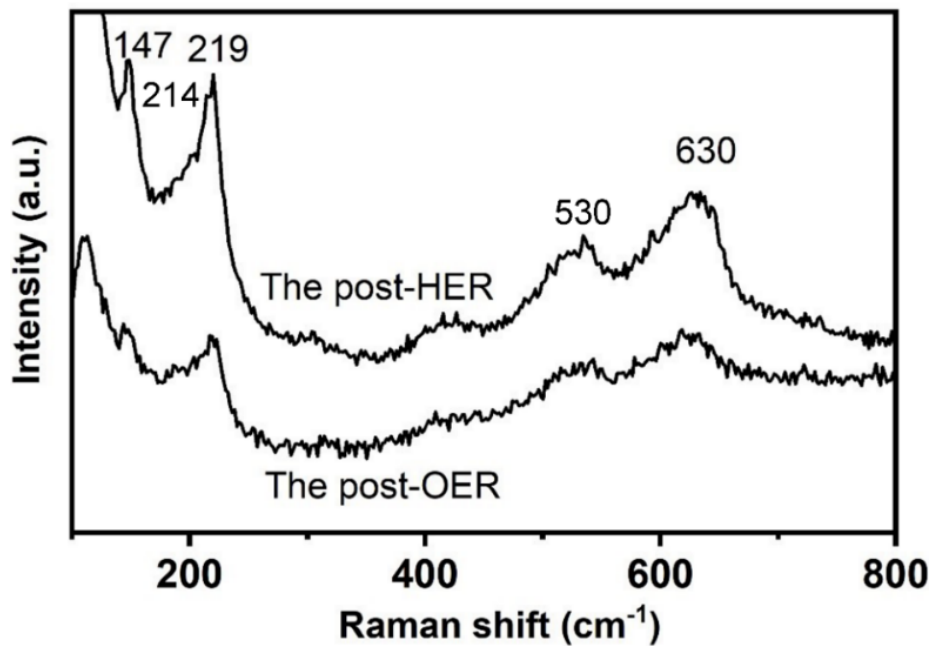
Figure S7. Raman spectra of FeSPPc/Cu$_x$O/CF after durability tests in electrocatalytic HER and OER, respectively.
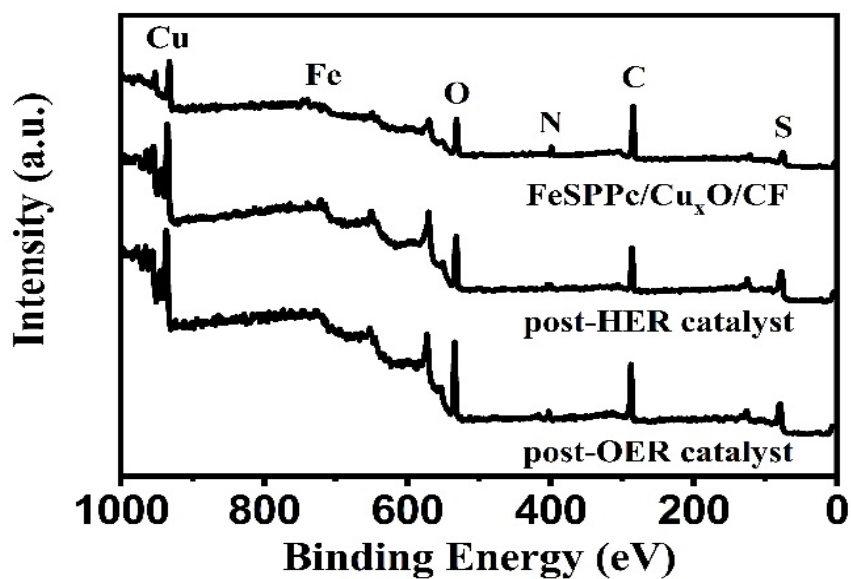
Figure S8. XPS survey spectra of FeSPPc/Cu$_x$O/CF before and after durability tests in electrocatalytic HER and OER.
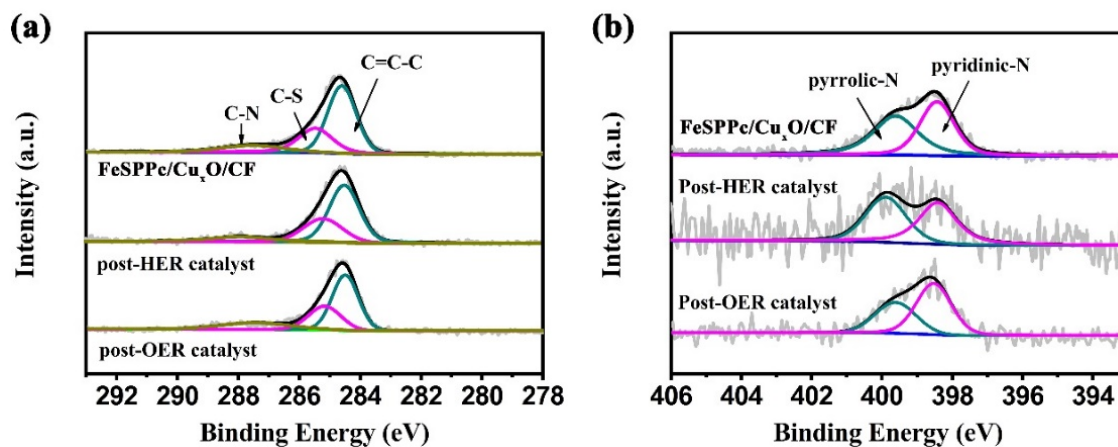
Figure S9. Comparison of XPS spectra of C 1s and N 1s peaks of FeSPPc/Cu$_x$O/CF before and after durability tests in electrocatalytic (a) HER and (b) OER, respectively.

Table S4. Comparison of the electrocatalytic performances of the material reported herein (FeSPPc/Cu$_x$O/CF) for HER, OER, and overall water splitting with other notable highly active electrocatalysts reported recently in the literature.

Catalyst	Support	η_a (mV)	η_b (mV)	CV (V)	Ref.
FeSPPc/Cu$_x$O/CF	CF	38 (η_{10})	350 (η_{10})	1.48	this work
Cu@NiFe LDH	CF	116 (η_{10})	199 (η_{10})	1.54	[2]
Ni/Cu/CF	CF	38 (η_{10})	-	1.51	[3]
CoN/Cu$_3$N	CF	134 (η_{10})	303 (η_{50})	1.62	[4]
Cu$_3$(PO$_4$)$_2$/Cu-BDC	CF	145 (η_{10})	241 (η_{10})	1.56	[5]
Cu@CoSx/CF	CF	267 (η_{100})	310 (η_{100})	1.50	[6]
Cu$_x$O NWs/CF	CF	135 (η_{10})	315 (η_{10})	-	[7]
Co-Cu$_3$P/CF	CF	200 (η_{50})	270 (η_{50})	1.55	[8]
Cu$_2$S-Co(OH)$_2$NTA/CF	CF	241(η_{10})	268 (η_{10})	1.55	[9]
Cu$_2$S@Cu	CF	316 (η_{10})	487 (η_{20})	1.84	[10]
Ru/Cu$_{2+1}$O NT/CuF	CF	32 (η_{10})	210 (η_{10})	1.53	[11]
CuO@Ni-PNA/CF	CF	106 (η_{30})	275 (η_{30})	1.71[*]	[12]
Ni$_3$S$_2$@MoS$_2$/FeOOH	CC	95 (η_{10})	234 (η_{10})	1.57	[13]
NiCo$_2$O$_4$@FeOOH/NF	NF	111 (η_{10})	187 (η_{10})	1.52	[14]
FeOOH/Ni$_3$N	NF	67 (η_{10})	244 (η_{10})	1.56	[15]
Cu$_3$N/NF	NF	118 (η_{10})	286 (η_{10})	1.62	[16]

η_a: The overpotential required by the material to electrocatalyze the HER at "a" mA cm^{-2}. η_b: The overpotential required by the material to electrocatalyze the OER at "b" mA cm^{-2}. CV: the cell voltage to afford 10 mA cm^{-2} toward overall water splitting in alkaline solution. [*]: the cell voltage to achieve 30 mA cm^{-2}.

Abbreviations: CC = carbon cloth; CF = copper foam; and NF = nickel foam.

References

[1] H. Chen, X. Huang, L.-J. Zhou, G.-D. Li, M. Fan, X. Zou, *ChemCatChem*, **2016**, *8*, 992-1000.

[2] Y. Luo, H. Zhou, J. Sun, F. Qin, F. Yu, J. Bao, Y. Yu, S. Chen and Z. Ren, *Energy Environ. Sci.,* 2017, **10**, 1820.

[3] S. Li, M. Li and Y. Ni, *Appl. Catal. B-Environ.*, 2020, **268**, 118392.

[4] J. Li, X. Kong, M. Jiang and X. Lei, *Inorg. Chem. Front.,* 2018, **5**, 2906.

[5] J. Rong, F. Qiu, T. Zhang, Y. Fang, J. Xu and Y. Zhu, *Electrochim. Acta,* 2019, **313**, 179.

[6] Y. Liu, Q. Li, R. Si, G. D. Li, W. Li, D. P. Liu, D. Wang, L. Sun, Y. Zhang and X. Zou, *Adv. Mater.*, 2017, **29**, 1606200.

[7] X. X. Ma, L. Chen, Z. Zhang and J. L. Tang, *Chin. J. Anal. Chem.*, 2020, **48**, 20001.

[8] Y. Rong, Y. Ma, F. Guo, J. Qian, H. Li, M. Zhou, Z. Xu, Y. Q. Zheng and T. T. Li, *Int. J. Hydrogen Energy,* 2019, **44**, 28833.

[9] D. Wang, J. Li, Y. Zhao, H. Xu and J. Zhao, *Electrochim. Acta*, 2019, **316**, 8.

[10] B. Ma, Z. Yang, Z. Yuan and Y. Chen, *Int. J. Hydrogen Energy,* 2019, **44**, 1620.

[11] J. Gao, L. Yang, D. Wang and D. Cao, *Chem. Eur. J.*, 2020, **26**, 4112.

[12] B. Chang, S. Hao, Z. Ye and Y. Yang, *Chem. Commun.*, 2018, **54**, 2393.

[13] M. Zheng, K. Guo, W. J. Jiang, T. Tang, X. Wang, P. Zhou, J. Du, Y. Zhao, C. Xu and J. S. Hu, *Appl. Catal. B-Environ.*, 2019, **244**, 1004.

[14] M. Li, L. Tao, X. Xiao, X. Lv, X. Jiang, M. Wang, Z. Peng and Y. Shen, *ChemCatChem*, 2018, **10**, 4119.

[15] J. Guan, C. Li, J. Zhao, Y. Yang, W. Zhou, Y. Wang and G. R. Li, *Appl. Catal. B-Environ.*, 2020, **269**, 118600.

[16] C. Panda, P. W. Menezes, M. Zheng, S. Orthmann and M. Driess, *ACS Energy Lett.*, 2019, **4**, 747.

[17] Z. N. Zahran, E. A. Mohamed, Y. Tsubonouchi, M. Ishizaki, T. Togashi, M. Kurihara, K. Saito, T. Yui and M. Yagi, *ACS Appl. Energy Mater.*, 2021, 4, 1410-1420.

[18] X. P. Wang, H. J. Wu, S. B. Xi, W. S. V. Lee, J. Zhang, Z. H. Wu, J. O. Wang, T. D. Hu, L. M. Liu, Y. Han, S. W. Chee, S. C. Ning, U. Mirsaidov, Z. B. Wang, Y. W. Zhang, A. Borgna, J. Wang, Y. H. Du, Z. G. Yu, S. J. Pennycook and J. M. Xue, *Energy & Environ. Sci.,* 2020, 13,

229-237.

[19] P. Zhang, L. Li, D. Nordlund, H. Chen, L. Fan, B. Zhang, X. Sheng, Q. Daniel and L. Sun, *Nat. Commun.*, 2018, 9, 381.

[20] X. Xu, F. Song and X. Hu, *Nat. Commun.*, 2016, 7, 12324.